A proteomic study on a human osteosarcoma cell line Saos-2 treated with diallyl trisulfide

Yong Kui Zhang[a], Xu Hua Zhang[b], Jian Min Li[c], De Sheng Sun[d], Qiang Yang[c] and Dong Mei Diao[e]

Garlic is generally used as a therapeutic reagent against various diseases, and numerous studies have indicated that garlic and its derivatives can reduce the risk of various types of human cancer. Diallyl trisulfide (DATS), a major member of garlic derivatives, could inhibit the cell proliferation by triggering either cell cycle arrest or apoptosis in a variety of cancer cell lines as shown in many studies. However, whether DATS has the same effect on human osteosarcoma cells remains unknown. In this study, we have attempted to analyze the effects of DATS on cell proliferation, cell cycle, induction of apoptosis, global protein expression pattern in a human osteosarcoma cell line Saos-2 cells, and the potential molecular mechanisms of the action of DATS. Saos-2 cells, a human osteosarcoma cell line, were treated with or without 25, 50, and 100 μmol/l DATS for various time intervals. The cell proliferation, cell cycle progression, and apoptosis were examined in this study. Then, after treatment with or without 50 μmol/l DATS for 48 h, protein add pattern in Saos-2 cells were systematically studied using two-dimensional electrophoresis and mass spectrometry. DATS could inhibit the proliferation of Saos-2 cells in a dose-dependent and time-dependent manner. Moreover, the percentage of apoptotic cell and cell arrest in G_0/G_1 phase was also dose-dependent and time-dependent upon DATS treatment. A total of 27 unique proteins in Saos-2 cells, including 18 downregulated proteins and nine upregulated proteins, were detected with significant changes in their expression levels corresponding to DATS administration. Interestingly, almost half of these proteins (13 of 27) are related to either the cell cycle or apoptosis. DATS has the ability to suppress cell proliferation of Saos-2 cells by blocking cell cycle progression and inducing apoptosis in a dose and time-dependent manner. The proteomic results presented, therefore, provide additional support to the hypothesis that DATS is a strong inducer of apoptosis in tumor cells. However, the exact molecular mechanisms, how these proteins significantly changed in the Saos-2 cell line upon DATS treatment, should be further studied.

Anti-Cancer Drugs 2009, **20:**702–712

Keywords: apoptosis, diallyl trisulfide, osteosarcoma, proteome

[a]Department of Orthopedics, Affiliated Hospital of Shandong University of Traditional Chinese Medicine, [b]Department of Clinical Laboratory, the Second Hospital of Shandong University, [c]Department of Orthopedics, Qilu Hospital of Shandong University, Jinan, [d]Department of Orthopedics, the People's Hospital of Penglai City, Penglai and [e]Department of Clinical Laboratory, the Maternity and Child Care Hospital of Yucheng City, Yucheng, China

Correspondence to Jian Min Li, Department of Orthopedics, Qilu Hospital of Shandong University, Jinan 250012, China
Tel: +86 531 82169423; fax: +86 531 82950414; e-mail: qlgkljm@sina.com

Received 13 January 2008 **Revised form accepted** 25 May 2009

Introduction

Numerous historical scientific data have indicated that garlic has therapeutic effects on various ailments such as heart disease, arthritis, pulmonary complaints, uterine growths, diarrhea, and worm infestation [1]. In addition, recent epidemiological studies have shown that garlic can reduce the risk of various types of human cancer [2]. The effect of garlic is primarily attributed to organosulfur compounds (OSCs), which are generated upon processing of garlic. Garlic-derived OSCs, including diallyl sulfide, diallyl disulfide, and diallyl trisulfide (DATS), have been shown to block carcinogenesis induced by a variety of chemical carcinogens at many sites, including skin, esophagus, lung, forestomach, mammary tissues, colon, and liver [3]. Extensive investigations have shown that the prevention of chemically induced cancers in animal models by OSCs was because of their ability to increase detoxification of activated carcinogenic metabolites through induction of phase II enzymes such as glutathione transferases and/or suppress carcinogen activation through inhibition of phase I enzymes [4–6]. Other recent studies have also shown that DATS could upregulate the expression of glutathione S-transferase related to the c-Jun N-terminal kinase–AP-1 and extracellular signal-regulated kinase–AP-1 signaling pathways [7].

Several studies have indicated that DATS could inhibit proliferation of cultured cancer cells by causing cell cycle arrest and inducing apoptosis. However, the mechanisms by which DATS takes its pharmacological effect on cell cycle and apoptosis are not fully defined. Moreover, it seems that the previous studies were limited to cancer cells from glandular organs or epithelial tissue. Xiao and Herman-Antosiewicz *et al.* [8,9] have shown that the DATS-induced cell cycle arrest in human prostate cancer cells was mediated by reactive oxygen species and was

0959-4973 © 2009 Wolters Kluwer Health | Lippincott Williams & Wilkins DOI: 10.1097/CAD.0b013e32832e89c7

associated with activation of checkpoint kinase 1. They have also provided experimental evidence to indicate that DATS-induced apoptosis in human prostate cancer cells was related to c-Jun *N*-terminal kinase and extracellular signal-regulated kinase-mediated phosphorylation of Bcl-2 as well as by inactivation of Akt leading to mitochondrial translocation of BAD (a proapoptotic protein) and activation of caspase 3 and 9 [10,11]. Other recent studies have also evidenced that OSCs, such as DATS, could cause cell cycle arrest and/or induce apoptosis in malignant tumor cells from human stomach, colon, lung, skin, and fibrous tissue [12–14].

Osteosarcoma is a primary malignant tumor of the skeleton characterized by the direct formation of immature bone or osteoid tissue by the tumor cells. The primary choice of adjunctive therapy for osteosarcoma is neoadjuvant chemotherapy. Although neoadjuvant chemotherapy is effective in improving patient survival, the frequent acquisition of drug-resistant phenotypes and the occurrence of 'second malignancy' are often associated with chemotherapy, which remain as serious problems [15]. Therefore, there is a clear need for new effective agents for patients with osteosarcoma. We attempted to apply DATS on human osteosarcoma cells and observed that the exposure to 150 μmol/l DATS led to significant morphological changes and a slow growth rate in Saos-2 cells, a human osteosarcoma cell line (data not shown). Now the challenge is how to elucidate the antineoplastic mechanisms of DATS, which may conduce to the development of chemotherapy for osteosarcoma.

Proteomics is an emerging field in medical science focused on the library of proteins specific to a given biosystem, the proteome, and understanding relationships therein. The proteomic strategy has provided the potentiality to profile the cellular responses at the protein level under stress, and it has been successfully used in the area of early detection and rational treatment of cancer [16]. Proteomic analysis of the human osteosarcoma cell lines has been reported by some investigators [15,17,18]. In our studies, the combination of two-dimensional electrophoresis (2-DE) with mass spectrometry and database interrogations allowed us to identify the proteins differentially expressed in Saos-2 cells after DATS treatment. Our data revealed that several cell cycle-associated or apoptosis-associated proteins in Saos-2 cells were expressed corresponding to DATS treatment. The information provided here, therefore, will deepen our knowledge on how DATS influences cell cycle arrest or apoptosis in cancer cells.

Materials and methods

Reagents

DATS was purchased from Shanghai Hefeng Pharmacy Company (Shanghai, China). Immobilized pH gradient (IPG) strips were obtained from Bio-Rad Laboratories (Hercules, California, USA). All chemical reagents for 2-DE were from Amersham Biosciences (Uppsala, Sweden), and HPLC grade solvents were acquired from J.T. Baker (Phillipsburg, New Jersey, USA). Trypsin and dimethyl sulfoxide (DMSO) were from Sigma (St. Lousis, Missouri, USA).

Cell culture and diallyl trisulfide treatment

Saos-2 cells were obtained from Institute of Biochemistry and Cell Biology (Shanghai, China). Cells were cultured in Dulbecco's modified Eagle's medium (Invitrogen, California, USA) containing 10% fetal bovine serum, 100 kU/l penicillin, and 100 mg/l streptomycin at 37°C in a humidified 5% CO_2 incubator. After a fraction of coverage reaching 60%, the cells were treated with 25, 50, or 100 μmol/l DATS. DATS was dissolved in 0.1% DMSO. Cells treated with DMSO alone were regarded as the control.

MTT assay

The effect of DATS on cell proliferation was measured by the MTT [3-(4-5dimethylthiozol-2-yl)-2,5-diphenyltetrazolium bromide] assay, based on the ability of live cells to convert thiazolyl blue to dark blue formazan. Exponentially growing cells were seeded into 96-well culture plates at 4×10^3 cells per well and treated with or without DATS for 24, 48, 72, and 96 h, respectively. After treatment, MTT (5 mg/ml) was added into each well for continual incubation at 37°C for 4 h and then DMSO was dropped in each well to dissolve the formazan product for 30 min at room temperature. A 96-well microplate reader (Rayto, USA) was used to measure the absorbance at 570 nm (A_{570}). At least three independent experiments were carried out.

Cell cycle analysis

After treatment with DATS at desired concentrations for various time intervals, both floating and adherent cells were collected, fixed with ice-cold 70% ethanol, and stored at −20°C before use. After being centrifuged and washed with phosphate-buffered solution (PBS), the cells were incubated with 1 mg/ml RNase A and stained with 50 μg/ml propidium iodide (PI). Then, FACSCalibur (Bethesda, USA) with Modfit software (Bio-Rad Laboratories, California, USA) was used for the analysis of cell cycle phase. At least three independent experiments were carried out.

Apoptosis analysis

Flow cytometry combined with annexin V/fluorescein isothiocyanate (FITC) Apoptosis Detection Kit (Bender, Austria) was used to determine the apoptosis of Saos-2 cells treated with DATS. Annexin V/FITC Apoptosis Detection Kit contains binding buffer, PI (20 μg/ml), and rh Annexin V/FITC. After being treated, the harvested cells were washed twice with precooling PBS and

resuspended in 250 μl binding buffer to modulate the cell concentration at 1×10^6/ml. Then, 100 μl of the cell suspension was pipetted into a 5 ml test tube, with 5 μl annexin V/FITC and 10 μl PI added to it. After this mixture had been incubated for 15 min at room temperature, 400 μl PBS was added to the test tube. Then, the apoptotic rate was analyzed on FACSCalibur. A cell isometric chart composed of four quadrants is required after analysis. In the cell isometric chart, the lower left quadrant, the lower right quadrant, upper right quadrant, and upper left quadrant represent normal (AnPI cells), earlier apoptotic (An + PI cells), secondary apoptotic (An + PI + cells), and necrotic (AnPI + cells) cells, respectively. The total number of apoptotic cells is the summation of earlier apoptotic cells and secondary apoptotic cells. At least three independent experiments were carried out.

Sample preparation for two-dimensional electrophoresis

After treatment with or without 50 μmol/l DATS for 48 h, the cells were harvested and washed three times using PBS, subsequently lysed with lysis buffer containing 40 mmol/l Tris, 7 mol/l urea, 2 mol/l thiourea, 4% (3-[(3-cholamidopropyl)dimethylammonio]-1-propanesulfonate), 40 mmol/l dithiotheritol (DTT), 1 mmol/l EDTA, 2% pharmalyte (pH 3–10), and 1 mmol/l phenylmethylsulfonyl fluoride. The suspension was sonicated with a probe sonicator for 5 min followed by centrifuging at 40 000*g* for 1 h. After quantification of proteins by the Bradford method, the supernatants were stored at −70°C until use for electrophoresis.

Two-dimensional electrophoresis

The protein sample of 150 μg was applied to 18 cm IPG stips (pH 3–10, nonlinear) and the strips were rehydrated for 12 h at 20°C. The isoelectric focusing was performed at 500 V for 1 h, at 1000 V for 1 h, and at 8000 V for 1 h, then, continued at 8000 V until a total of 50 kVh. After the first dimension, the focused strips were equilibrated for 15 min in the buffer containing 6 mol/l urea, 30% glycerol, 2% SDS, 1% DTT, and trace bromophenol blue, then for 15 min in the same buffer containing 2.5% iodoacetamide instead of DTT. After equilibration, the strips were loaded on 12% SDS–polyacrylamide gels running at 2.5 W each gel for 30 min and 15 W each gel until the bromophenol blue dye reached the bottom of the gel. Then, the gels were treated by silver staining. Triplicate gels for each sample were performed to achieve reproducible results.

The gels were scanned by Imagescanner (Amersham Bioscience, Sweden) and the image analysis was performed with ImageMaster 2D Platinum (Amersham Bioscience). The spot volume is described as the multiplied area of a spot and the intensity inside this area. The threshold of the significant change in 2-DE spots was defined as a three-fold change in spot volume upon comparison of average gels between the treated and control groups.

Mass spectrometry

The gel spots verified as the significant changes in spot volume were separated by picker P2D1.5 (San Francisco, USA) and transferred into Eppendorf tubes. The particles were treated with reduction of DTT and alkylation of iodoacetamide followed by a thorough process of washing and drying. Then, the treated gel particles were incubated in 20 μl of 25 mmol/l NH_4HCO_3 containing 0.05 μg/μl trypsin at 37°C overnight. After centrifuging, the supernatants were mixed with 2 μl of 5% trifluoroacetic acid and delivered to mass spectrometry.

The tryptic digests were desalted by POROS R2 (Applied Biosystems, California, USA), and cocrystallized with a matrix of α-cyano-4-hydroxycinnamic acid spotted on the target wells. Then, the dried matrix was subjected to a Bruker autoflex matrix-assisted laser desorption ionization time-of-flight mass spectrometry (MALDI-TOF MS) (Bremen, Germany). The mass spectrometer was operated at 19 kV accelerating voltage in the reflectron mode and the *m/z* range was from 600 to 4000. All peptide mass fingerprints were externally calibrated using standard peptide mixtures and internally calibrated using the masses of tryptic autolysis products. The monoisotopic peptide masses obtained from MALDI-TOF MS were analyzed by *m/z* software, and interpreted by Mascot (Matrix Science, Massachusetts, USA) against the NCBInr database in which one incomplete fragment was allowed and alkylation of cysteine by carbamidomethylation oxidation of methionine and pyro-Glu formation of *N*-terminal Gln were considered as possible modifications.

Statistical analysis

Values were expressed as mean ± SD and analyzed by one-way analysis of variance and the Fisher's least significant difference test to determine significant differences among group means ($P < 0.05$).

Results

MTT assay

The antiproliferative effect of DATS on a human osteosarcoma cell line, Saos-2 cells, was examined by exposing them to different concentrations of DATS (25, 50, or 100 μmol/l) for 24, 48, 72, and 96 h, respectively. The rates of cell growth were detected by MTT assay as shown in Fig. 1, in which 100 μmol/l DATS inhibited Saos-2 cell proliferation in 24 h treatment, and 50 μmol/l in 48 h treatment. However, a significant inhibition of cell growth was observed until 72 h of incubation with 25 μmol/l DATS. The inhibitive effect of DATS on cell growth was increased with the prolonged treatment time.

Cell cycle analysis

As shown in Fig. 2, the Saos-2 cells were arrested at G_0/G_1 phase when the cells were treated with DATS for 48 h. Furthermore, the higher the concentration of DATS used, the more Saos-2 cells were blocked at G_0/G_1 phase (Table 1). In addition, the cells also showed a time-dependent arrest at G_0/G_1 phase when exposed to 50 μmol/l DATS (Fig. 3). Table 2 shows the effects of 50 μmol/l DATS on the cell cycle after treatment for 24, 48, 72, and 96 h, respectively. According to the results shown in Table 2, the percentage of cells arrested at G_0/G_1 phase in 50 μmol/l DATS-treated groups was significantly higher than the control ($P < 0.05$). As the treatment time increased, the percentage of cells arrested at G_0/G_1 phase also increased.

Fig. 1

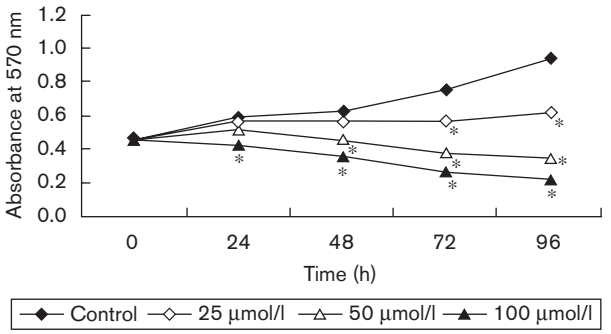

Diallyl trisulfide (DATS) inhibited the proliferation in Saos-2 cells. The Saos-2 cells were treated with 25, 50, or 100 μmol/l of DATS for 24, 48, 72, and 96 h, respectively. Cells treated with dimethyl sulfoxide alone were regarded as the control. After treatment, the cells were exposed to MTT assay as described in Material and methods. Asterisks indicate the significant inhibition of cell growth ($P < 0.05$).

Apoptosis analysis

Figure 4 shows that DATS can induce apoptosis in Saos-2 cells. After treatment with 100 μmol/l DATS for 48 h, the percentage of apoptotic cells ($36.92 \pm 0.65\%$) was significantly higher than the 25 μmol/l group ($11.62 \pm 0.90\%$) and the 50 μmol/l group ($22.15 \pm 0.79\%$) (Table 3) ($P < 0.05$). It is shown that DATS can induce apoptosis in a dose-dependent manner. Furthermore, the effect of DATS-induced apoptosis is increased in a time-dependent manner (Fig. 5). Table 4 also shows the effects of 50 μmol/l DATS on apoptosis after treated for 24, 48, 72, and 96 h, respectively. As shown in Table 4, 50 μmol/l DATS time dependently induced apoptosis of Saos-2 cells.

Two-dimensional electrophoresis pattern

In this study, we used 2-DE in conjunction with quantitative image analysis and sequencing mass spectrometry to investigate the changes of protein expression in Saos-2 cells treated with or without DATS. A 2-DE protein map

Table 1 Effect of 25, 50, 100 μmol/l DATS on cell cycle of Saos-2 cells

Group	G_0/G_1 (%)	G_2/M (%)	S (%)
Control	40.94 ± 1.36^a	17.81 ± 1.12^b	40.95 ± 1.79^c
25 μmol/l	42.08 ± 1.84^a	20.09 ± 2.00^b	37.83 ± 1.91^c
50 μmol/l	55.66 ± 1.87	19.48 ± 0.62^b	24.86 ± 1.35
100 μmol/l	63.30 ± 2.55	17.79 ± 3.12^b	18.98 ± 1.69
F value	173.93	0.91	109.81

Saos-2 cells were cultured in Dulbecco's modified Eagle's medium containing 25, 50, and 100 μmol/l DATS for 48 h, respectively. Cells treated with DMSO alone for 48 h were regarded as the control. Values are expressed as means ± SD of four separate experiments.
DATS, diallyl trisulfide; DMSO, dimethyl sulfoxide.
[a,b,c]Groups sharing the same superscript letter are not significantly different from one another ($P < 0.05$) by one-way analysis of variance and least significant difference test.

Fig. 2

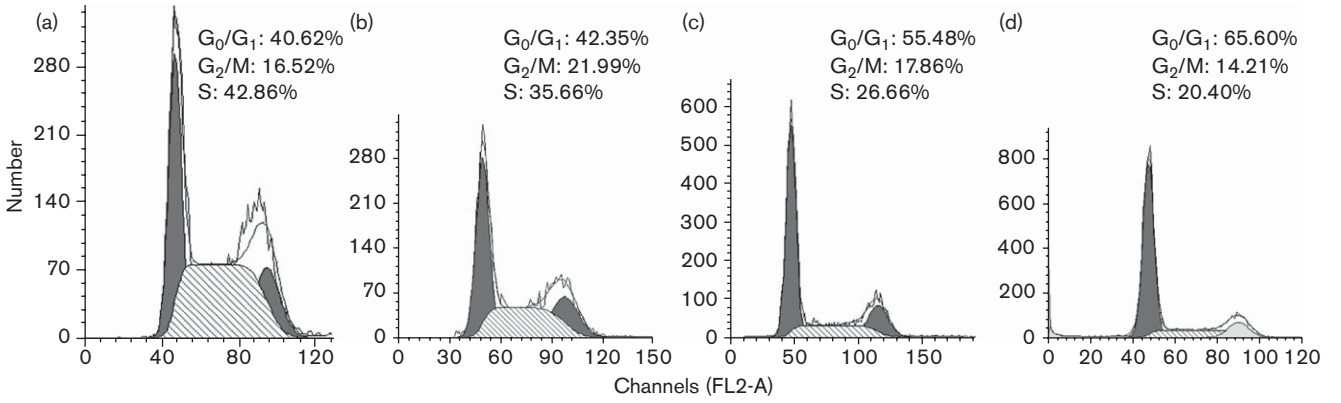

Effect of 25, 50, and 100 μmol/l diallyl trisulfide (DATS) on the cell cycle of Saos-2 cells. (a–d) Saos-2 cells were treated for 48 h with dimethyl sulfoxide, 25, 50, or 100 μmol/l DATS, respectively.

Fig. 3

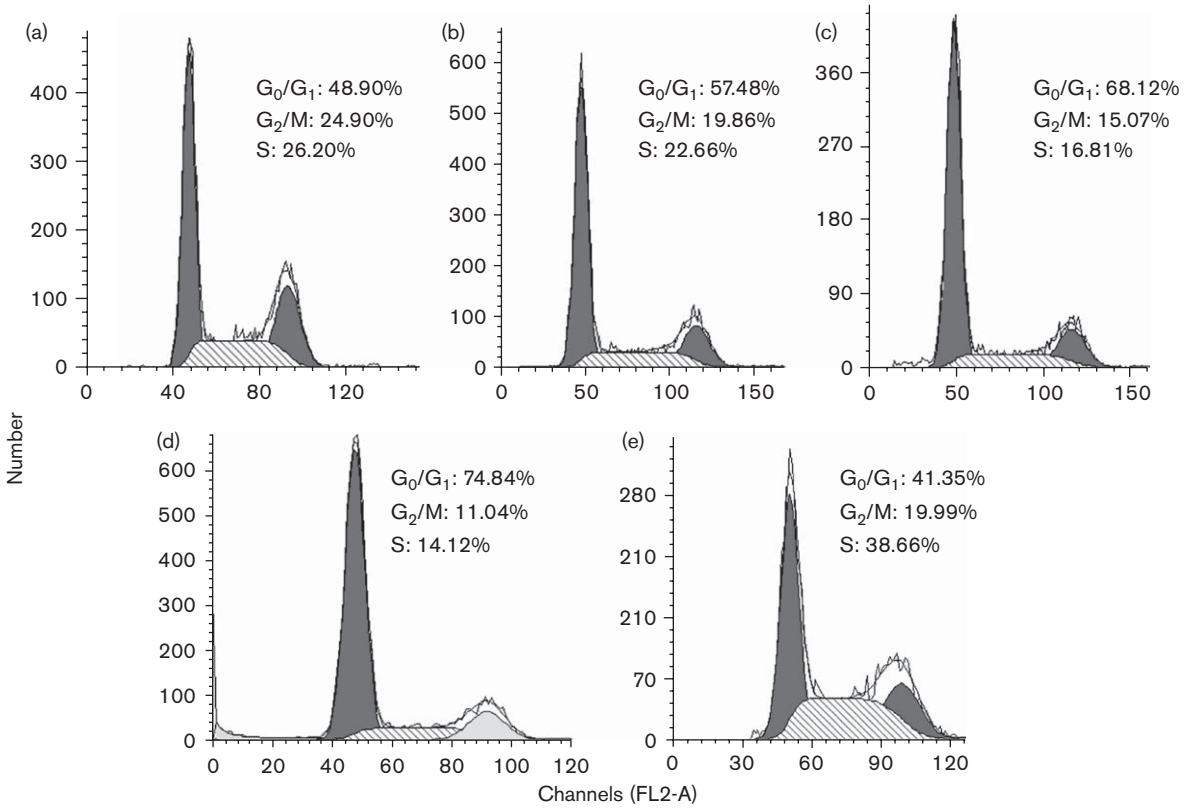

Effect of 50 μmol/l diallyl trisulfide (DATS) on the cell cycle of Saos-2 cells for various time intervals. (a–d) Saos-2 cells were treated with 50 μmol/l DATS for 24, 48, 72, and 96 h, respectively. (e) Saos-2 cells treated with dimethyl sulfoxide alone for 48 h was regarded as the control.

Table 2 Effect of 50 μmol/l DATS on cell cycle of Saos-2 cells during different incubation time intervals

Groups	Time (h)	G_0/G_1 (%)	G_2/M (%)	S (%)
Control	48	40.86 ± 0.49^a	20.09 ± 1.33^b	39.05 ± 0.78^d
50 μmol/l	24	48.61 ± 1.04^a	$24.27 \pm 0.65^{b,c}$	27.12 ± 1.11^d
	48	56.32 ± 1.32^a	20.82 ± 2.35^c	22.86 ± 1.36^d
	72	67.46 ± 0.58^a	$16.01 \pm 1.07^{b,c}$	16.53 ± 0.84^d
	96	74.38 ± 1.81^a	$12.29 \pm 1.54^{b,c}$	13.33 ± 0.96^d
F value		417.47	33.54	318.59

Saos-2 cells were cultured in Dulbecco's modified Eagle's medium containing 50 μmol/l DATS for 24, 48, 72, and 96 h, respectively. Cells treated with DMSO alone for 48 h were regarded as the control. Values are expressed as means ± SD of four separate experiments.
DATS, diallyl trisulfide; DMSO, dimethyl sulfoxide.
[a,b,c,d]Groups sharing the same superscript letter are significantly different from one another ($P < 0.05$) by one-way analysis of variance and least significant difference test.

was considered as a prerequisite for subsequent comparative proteomic studies. As DATS used for cell culture was dissolved in DMSO, the experiments of quality control were always conducted to ensure whether low concentration of DMSO contributed any side effect to the protein expression in Saos-2 cells. The image analysis of 2-DE showed that the patterns of electrophoretic spots were homoplastic in two media with or without 0.1% DMSO (data not shown) and the total spots were 321 ± 5 ($n = 3$, without 0.1% DMSO) and 316 ± 6 ($n = 3$, 0.1% DMSO), respectively. This result indicated that 0.1% DMSO had no obvious regulatory effect on the protein expression of Saos-2 cells.

We selected a reference gel against which each of the other gel images was matched. Three gels per sample underwent automatic spot detection and manual editing before automatic spot matching both within and between groups. Manual matching was done where necessary. Base-paired normalization was done on all the gels before examination of spot volume data. Gels were normalized in accordance with ImageMaster software protocols using base-paired normalization. Figure 6 shows the 2-DE images for Saos-2 cells cultured in the absence and presence of DATS. On the 2-DE images, the proteins in Saos-2 cells either with or without DATS treatment showed electrophoretically in similar modes along molecular mass and pI. The spots were biased toward the specific pH regions on the IPG strips, whereas they were evenly distributed over the range of molecular mass from 10 to 100 kDa on 12% SDS–polyacrylamide gel. The total spots were 316 ± 6 ($n = 3$) and 310 ± 3 ($n = 3$) in the

Fig. 4

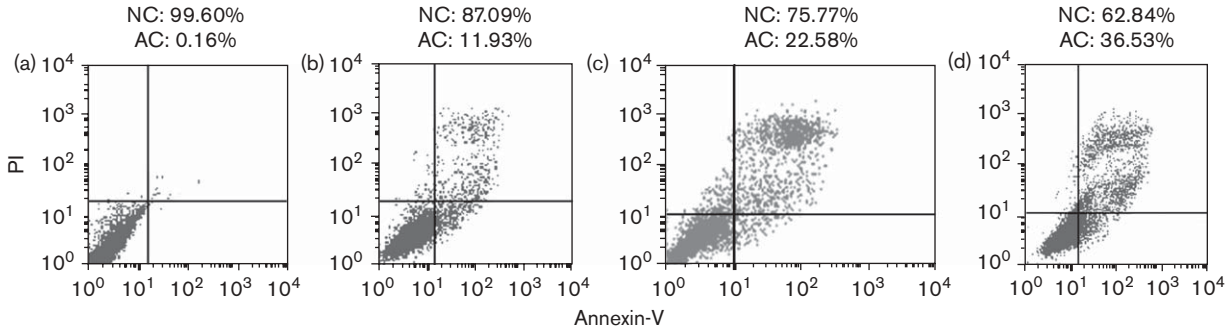

Effect of 25, 50, and 100 μmol/l diallyl trisulfide (DATS) on the apoptosis of Saos-2 cells. (a–d) Saos-2 cells were treated for 48 h with dimethyl sulfoxide, 25, 50, or 100 μmol/l DATS, respectively. AC, apoptotic cells; NC, normal cells; PI, propidium iodide.

Table 3 Effect of 25, 50, and 100 μmol/l DATS on cell apoptosis of Saos-2 cells

Group	IC (%)	AC (%)	NC (%)
Control	0.28 ± 0.07	0.23 ± 0.06[a]	99.49 ± 0.10[b]
25 μmol/l	0.56 ± 0.23	11.62 ± 0.90[a]	87.82 ± 0.99[b]
50 μmol/l	1.14 ± 0.44	22.15 ± 0.79[a]	77.04 ± 1.58[b]
100 μmol/l	0.90 ± 0.19	36.92 ± 0.65[a]	62.18 ± 0.82[b]
F value	2.06	781.79	356.19

Saos-2 cells were cultured in Dulbecco's modified Eagle's medium containing 25, 50, and 100 μmol/l DATS for 48 h, respectively. Cells treated with DMSO alone for 48 h were regarded as the control. Values are expressed as means ± SD of four separate experiments.
AC, apoptotic cells; DATS, diallyl trisulfide; DMSO, dimethyl sulfoxide; IC, impaired cells; NC, normal cells.
[a,b]Groups sharing the same superscript letter are significantly different from one another ($P < 0.05$) by one-way analysis of variance and least significant difference test.

control and DATS-treated groups, respectively. Of these proteins with molecular masses ranging from 10 to 100 kDa, approximately 70% had acidic pIs, whereas 30% of polypeptide spots fell within the alkaline region. There were few protein spots over 100 kDa, and few spots were detected with a pI of greater than 9. A total of 36 spots were defined as DATS-sensitive in Saos-2 cells, including 22 downregulated spots and 14 upregulated spots.

Identification of differentially expressed proteins

Stringent criteria for mass spectrometry were adopted to ensure the accuracy of protein identification: (π) the identified protein must rank at the top two hits with at least five matched sequences and (θ) the total coverage must be greater than 10%. The spots from the 2-DE gel were subjected to trypsin digestion and MALDI-TOF MS analysis. On the basis of the mass spectrometry data, 36 spots matched with the proteins, in which 27 spots were ascertained as unique proteins including 18 downregulated and nine upregulated (Tables 5 and 6) protiens. These proteins are involved in many biological functions, such as cell growth and apoptosis, cell differentiation and mobility, cell structure and basic metabolism, protein biosynthesis and degradation. In our study, the DATS-sensitive proteins, which may be involved in the cell cycle arrest or apoptotic pathway are listed in Table 7.

Discussion

In this study, we have investigated the effects of DATS on a human osteosarcoma cell line, Saos-2 cells. The results show that the percentage of apoptotic cells and cells arrested in G_0/G_1 phase were dose and time-dependent on DATS treatment. In an effort to detect the change of protein expression in human osteosarcoma cell, we used 2-DE and mass spectrometry to examine the protein profiles of Saos-2 cells treated with or without DATS. The data show that 36 spots were defined as proteins with 27 unique ones, in which almost half of these proteins (13 of 27) are related to either cell cycle or apoptosis.

In the last decade, the regulation of apoptosis or cell cycle has been considered as a significant strategy for cancer therapy. Several groups have reported that DATS could cause cell cycle arrest at G_2/M phase in cancer cells, and this effect may be associated with reactive oxygen species, checkpoints kinase 1, cyclin-dependent kinase 1,7, cyclinB 1 kinase, and Cdc 25C protein [8,9,19,20]. In our study, the results indicate that DATS can cause cell cycle arrest of Saos-2 cells at G_0/G_1 phase in a dose- and time-dependent manner. Furthermore, we ascertained that the expression of proteasome and keratin 10 could be downregulated or upregulated by DATS. The proteasome plays a pivotal role in the cellular housekeeping by eliminating mutant, misfolded, and damaged proteins. Moreover, the proteasome is involved in the targeted elimination of regulatory proteins, such as transcription factors, signaling molecules, and cell cycle inhibitors [21]. Thus, any inhibition of the proteasome system creates an imbalance of various regulatory proteins, triggering cell cycle arrest at G_1/S and G_2/M phases or apoptosis [22]. The therapeutic

Fig. 5

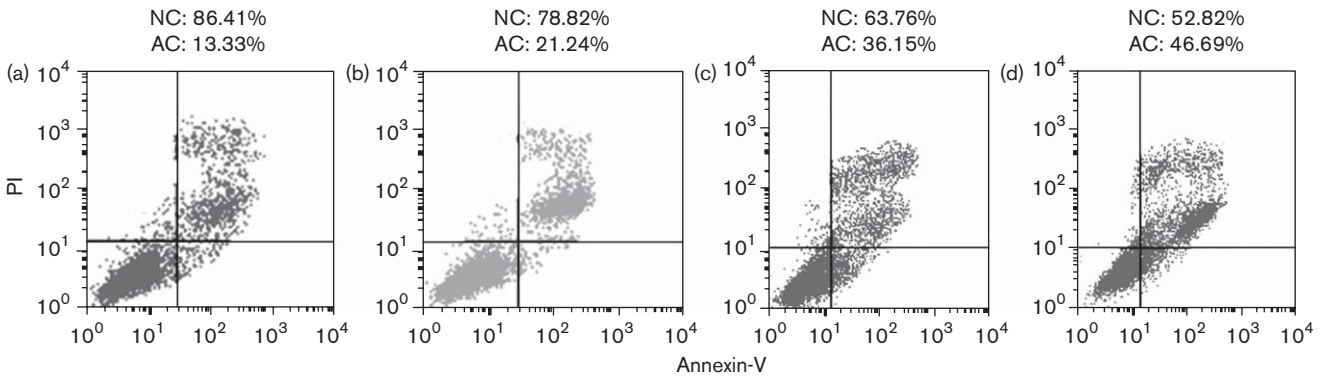

Effect of 50 μmol/l diallyl trisulfide (DATS) on the apoptosis of Saos-2 cells for various time intervals. (a–d) Saos-2 cells were treated with 50 μmol/l DATS for 24, 48, 72, and 96 h, respectively. AC, apoptotic cells; NC, normal cells; PI, propidium iodide.

Table 4 Effect of 50 μmol/l DATS on cell apoptosis of Saos-2 cells during different incubation time intervals

Group	Time (h)	IC (%)	AC (%)	NC (%)
50 μmol/l	24	0.68 ± 0.36	13.63 ± 1.19[a]	84.93 ± 1.15[b]
	48	1.14 ± 0.44	22.15 ± 0.79[a]	77.04 ± 1.58[b]
	72	1.10 ± 0.25	35.66 ± 0.42[a]	63.13 ± 0.51[b]
	96	0.66 ± 0.15	47.91 ± 1.53[a]	51.44 ± 1.59[b]
F value		2.05	598.03	396.09

Saos-2 cells were cultured in Dulbecco's modified Eagle's medium containing 50 μmol/l DATS for 24, 48, 72, and 96 h, respectively. Values are expressed as means ± SD of four separate experiments.
AC, apoptotic cells; DATS, diallyl trisulfide; DMSO, dimethyl sulfoxide; IC, impaired cells; NC, normal cells.
[a,b]Groups sharing the same superscript letter are significantly different from one another ($P < 0.05$) by one-way analysis of variance and least significant difference test.

value of proteasome inhibitor in human malignancy has recently shown significant preclinical and clinical activity in several cancers [23–25]. Moreover, bortezomib, a proteasome inhibitor had been approved in 2003 for the treatment of advanced multiple myeloma [22]. Several previous studies suggested that keratin 10 could inhibit cell proliferation by reducing cyclin D1 expression and thus retinoblastoma protein phosphorylation that controlled cell cycle progression during G_1 [26] and these effects were because of the interaction of keratin 10 with Akt and PKCς, critical effectors of the PI-3K pathway [27]. In addition, proteosome interacted with keratins in a cell cycle-dependent manner, which is involved in the control of cell cycle and signal transduction processes [28]. By using 2-DE and mass spectrometry, we confirmed that DATS can inhibit or induce the expression of proteasome and keratain 10, which may be associated with the cell cycle arrest of Saos-2 cells at G_0/G_1 phase.

Three biological processes, including mitochondrial signals, calcium homeostasis, and oxidative stress, are typical events that result in or from apoptosis [12]. Several components of apoptotic pathways have been widely investigated under DATS-induction, such as upregulation of Bax, Bad or Bak, downregulation of Bcl-2, activation of caspase-3 and caspase-9 [10,29]. Corresponding to these alterations, naturally, a network response related to apoptosis in Saos-2 cells treated with DATS can be expected.

Glucose-regulated protein 78 (GRP78), also known as BiP protein, is a major endoplasmic reticulum (ER) chaperone with Ca^{2+}-binding and antiapoptotic properties [30]. Several studies indicated that GRP78 can promote tumor proliferation, survival, metastasis, and resistance to a wide variety of therapies, and some components of apoptotic pathways or other signal pathways, such as PKC-ε/ERK/AP-1 signaling cascade, inhibition of caspase-7, prevention of Bax activation, were involved [31–34]. Thus, GRP78 expression may serve as a biomarker for tumor behavior and treatment response. In addition, recent investigations have verified that targeting GRP78 could promote apoptosis or overcome resistance to drug-induced cell death in several cancer cells [32,33,35,36]. Heat shock proteins (HSPs) are molecular chaperones, which are the biochemical regulators of cell growth, apoptosis, protein homeostasis, and cellular targets of peptides. Hsp70 and its co-chaperones, especially the Bcl-2-associated proteins, are well-recognized antiapoptotic factors [37]. Recent studies have shown that Hsp70 blocks the assembly of a multiprotein complex, which is essential for activating caspases that are responsible for executing the apoptotic program [38,39], and enforced overexpression of Hsp70 in transfected cells provided protection from stress-induced apoptosis at the levels of both cytochrome c release and caspase inactivation [38]. Although we observed that DATS can downregulate the expressions of GRP78/BiP and HSP70, the molecular mechanisms on how the expression and function of

Fig. 6

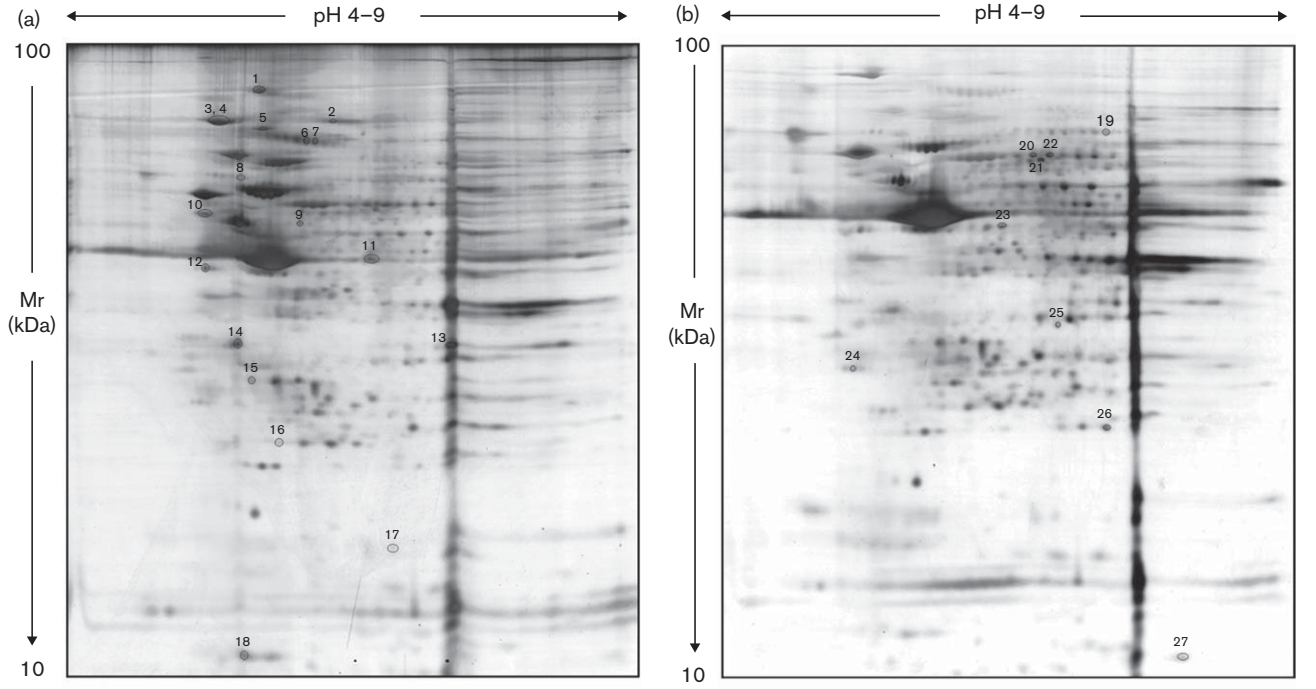

Images of two-dimensional electrophoresis (2-DE) for the proteins extractions of Saos-2 cells. The Saos-2 cells were treated without (a) or with 50 μmol/l diallyl trisulfide (b) for 48 h, respectively, followed by 2-DE analysis. Triplicate gels for each sample were performed to achieve reproducible results.

Table 5 Downregulated proteins in Saos-2 cells treated with DATS

Code	Accession no.	Description	Mr (kDa)	pI	Score	Sequence coverage (%)	Fold change
1	gi|5453832	150 kDa oxygen regulated protein precursor	111.49	5.16	223	35	0.110
2	gi|21264428	Stress-70 protein, mitochondrial precursor (75 kDa glucose-regulated protein)	73.92	5.87	190	45	– ∞
3	gi|4916999	78 kDa glucose-regulated protein	72.40	5.07	264	52	0.250
4	gi|1143492	BIP	72.18	5.03	302	60	0.175
5	gi|5729877	Heat shock 70 kDa protein 8 isoform 1	71.08	5.37	163	37	– ∞
6	gi|190127	Mitochondrial matrix protein	61.19	5.70	152	44	0.152
7	gi|41399285	Chaperonin (Homo sapiens)	61.18	5.70	150	45	0.277
8	gi|306890	Chaperonin (HSP60)	61.15	5.07	126	41	0.334
9	gi|90110780	Nucleobindin-1 precursor (CALNUC)	53.85	5.15	76	37	0.314
10	gi|55977767	Vimentin	53.67	5.06	205	69	– ∞
11	gi|4501887	Actin, γ-1 propeptide (Homo sapiens)	42.05	5.29	155	45	0.318
12	gi|119590557	Heat shock 60 kDa protein 1 (chaperonin),	41.06	5.09	76	33	0.117
13	gi|130848	Proteasome subunit C2	29.82	6.15	82	34	– ∞
14	gi|130848	Proteasome subunit alpha type 1	29.82	5.10	82	34	– ∞
15	gi|4185720	Ubiquitin carboxy-terminal hydrolase L1	23.35	5.30	73	31	0.278
16	gi|119631974	hCG1647962, isoform CRA_b	22.76	5.17	31	11	– ∞
17	gi|119621140	Ras-associated protein Rap1	20.53	7.12	29	21	0.296
18	gi|82408041	Chain B, solution Nmr structure of protein dynein light chain 2a	12.14	5.20	24	37	– ∞

The accession numbers were obtained from Matrix Science (*http://www.matrixscience.com*) using the Mascot peptide mass fingerprint program.
BIP, immunoglobulin-binding protein; DATS, diallyl trisulfide.

GRP78/BiP and HSP70 are mediated by DATS remain to be elucidated in future studies.

Alteration of actin remodeling not only plays an important role in regulating the morphologic and phenotypic events of a malignant cell, but also provides a potential target for anticancer drug development [40]. Verrills *et al.* [41] defined γ-actin as an essential factor in the efficacy of antimicrotubule agent therapy and suggested that drug resistance in human acute lymphoblastic leukemia cells involve the interaction between γ-actin and microtubules. In this study, the expression of γ-actin was

Table 6 Upregulated proteins in Saos-2 cells treated with DATS

Code	Accession no.	Description	Mr (kDa)	pI	Score	Sequence coverage (%)	Fold change
19	gi|62089214	ALPL protein variant	66.52	6.86	89	32	3.201
20	gi|127801853	Alkaline phosphatase	57.61	6.19	132	30	5.254
21	gi|127801853	Alkaline phosphatase, liver/bone/kidney	57.61	6.19	163	41	6.720
22	gi|116734717	Tissue nonspecific alkaline phosphatase precursor	57.61	6.19	161	43	6.187
23	gi|20141266	Alpha-internexin (α-Inx) (66 kDa neurofilament protein)	55.52	5.34	107	34	∞
24	gi|62897681	Calreticulin precursor (Homo sapiens)	47.06	5.02	50	21	∞
25	gi|186629	Keratin 10	39.83	5.72	70	25	5.728
26	gi|5716475	Phosphofructokinase, platelet-type	23.15	7.59	41	27	6.180
27	gi|119599010	hCG1644186 (Homo sapiens)	10.70	7.52	50	21	∞

The accession numbers were obtained from Matrix Science (*http://www.matrixscience.com*) using the Mascot peptide mass fingerprint program.
DATS, diallyl trisulfide.

Table 7 DATS-sensitive proteins in Saos-2 cells may be involved in cell cycle arrest or apoptotic pathways

Protein	Biological function	Expression level	Reference
Proteasome	Inhibits cell cycle arrest and apoptosis via ubiquitin-proteasome pathway	Down	[22]
GRP 78/BIP	Plays a key role in a survival response against drug-induced apoptosis by preventing Bax activation	Down	[34]
Heat shock 70 kDa protein (HSP70)	Provides protection from stress-induced apoptosis at the levels of both cytochrome c release and initiator caspase activation	Down	[38]
γ-actin	Inhibits antimicrotubule agent-induced cell death	Down	[41]
Ras-associated protein-1	Involved in the activation of MAPK pathway and integrin activation in human melanoma cells	Down	[43]
Vimentin	Associated with a dedifferentiated malignant phenotype, increased motility, invasive ability and poor prognosis	Down	[54]
Oxygen-regulated protein	Inhibits celecoxib-induced apoptosis	Down	[63]
Ubiquitin carboxy-terminal hydrolase L1	Prevents ischemia-induced retinal cell apoptosis	Down	[64]
Keratin 10	Induces cell cycle arrest because of the interaction of keratin 10 with Akt and PKCζ	Up	[27]
Alpha-internexin	Induces apoptosis-like cell death in PC12 cells	Up	[59]
Calreticulin	Induces apoptosis by increasing the concentration of cytosolic free Ca^{2+}	Up	[50]
Alkaline phosphatase, liver/bone/kidney	Reduces secretion of matrix metalloproteinase-9 enzyme and inhibits tumorigenic and metastatic ability in U-2OS cells	Up	[60]
Tissue nonspecific alkaline phosphatase	Promotes formation of hydroxyapatite crystals in osteoblast matrix vesicles and then propagates them into the extracellular matrix	Up	[61]

BIP, immunoglobulin-binding protein; DATS, diallyl trisulfide.

downregulated by DATS, which is the first report on γ-actin in a human osteosarcoma cell line. Rap1 is a member of the Ras family of small GTPases that is activated by diverse extracellular stimuli in many cell types. Functionally, Rap1 interferes with Ras-mediated ERK activation or activates ERK independent of Ras in a cell-context-dependent manner, and is involved in the activation of MAPK pathway and integrin, which suggest a potential role of Rap1 in tumorigenesis and metastasis [42,43]. Most recently, significant evidence has emerged that enhanced activation of Rap1 is responsible for transformed phenotype and increased invasiveness of cancer cells [44,45]. Corresponding to these outcomes, the data in this study show that DATS can downregulate the expression of Rap1 in Saos-2 cells, but its functional mechanism remains to be illuminated.

Both Ca^{2+} signaling and Ca^{2+} homeostasis provide critical environment for apoptosis. Garlic derivatives have been observed to interfere in Ca^{2+} homeostasis and activate Ca^{2+}-dependent endonucleases and apoptosis [14]. When HCT15 cells were treated with diallyl disulfide, an increase in intracellular calcium level was correlated with cell cycle arrest and apoptosis induction [46]. Similar effects were observed in lung cancer cells exposed to DATS [47]. In this study, several DATS-sensitive proteins in Saos-2 cells are believed to participate in the regulation of Ca^{2+}, such as GRP78/BiP and calreticulin. GRP78/BiP is a major ER chaperone with Ca^{2+}-binding and antiapoptotic properties [30], and its expression can be dramatically enhanced with Ca^{2+} ionophores [48]. However, more studies should be carried out to elucidate the exact correlation of GRP78/BiP and intracellular Ca^{2+} in the apoptotic pathway. Calreticulin is also an ER protein with several unique functions, including chaperone activity and regulation of Ca^{2+} homeostasis [49]. Arnaudeau *et al.* [50] observed that calreticulin overexpression increased Ca^{2+} fluxes across ER but decreased mitochondrial Ca^{2+} and membrane potential. Thus, increased Ca^{2+} turnover between the two organelles might damage mitochondria, accounting for the increased susceptibility of cancer cells to apoptotic stimuli. Several studies have shown that calreticulin-overexpressing cancer cells showed increased sensitivity to drug-induced or radiation-induced apoptosis [51,52], whereas calreticulin-deficient cells were more resistant to ultraviolet radiation-induced apoptosis [53]. Moreover, the overexpression of calreticulin can modulate

radiation-induced apoptosis by suppressing Akt signaling and regulating p53 function through altered Ca^{2+} homeostasis [52,53]. Taken together, Ca^{2+} signaling and Ca^{2+} homeostasis modulated by GRP78/BiP and calreticulin are plausible to explain this apoptotic process induced by DATS in Saos-2 cells.

Interestingly, vimentin, one of the cytoskeletal proteins, was significantly decreased in Saos-2 cells stimulated with DATS. Vimentin is often associated with dedifferentiated malignant phenotype, increased motility, invasive or metastatic ability, and poor prognosis in cancer cells [54,55]. In addition, vimentin can be cleaved by caspases-3, 6, and 7 during apoptosis, and its proteolysis promotes apoptosis by dismantling intermediate filaments and generating a proapoptotic aminoterminal cleavage product [56]. Moreover, reducing vimentin expression could lead to a significant decrease in the invasive ability of cancer cells [54,57]. α-internexin, an intermediate filament protein that is expressed in normal neurons undergoing maturation and differentiation, was first found to be significantly upregulated after DATS treatment in Saos-2 cells. It was previously shown that α-internexin was expressed in medulloblastomas and atypical teratoid–rhabdoid tumors [58], and induced apoptosis-like cell death in a rat adrenal pheochromocytoma cell line, PC12 cells [59].

Alkaline phosphatases are a family of glycoproteins that are able to hydrolyze various monophosphate esters at a high pH optimum. Liver/bone/kidney (L/B/K) alkaline phosphatase (ALP) and tissue nonspecific alkaline phosphatase (TNSALP) are two of the four major isoenzymes that belong to this family. L/B/K ALP expression can reduce secretion of matrix metalloproteinase-9 enzyme and inhibit tumorigenic and metastatic ability in U-2OS cells [60]. As a well-known indicator of bone formation, TNSALP may initiate and/or promote formation of hydroxyapatite crystals in osteoblast matrix vesicles and then propagate them into the extracellular matrix [61]. Several studies indicated that all-trans-retinoic acid could upregulate TNSALP expression and catalytic activity, which were correlated with the inhibition of malignant tumor cell proliferation [61,62]. In this study, the expression of L/B/K ALP and TNSALP can be upregulated by DATS in Saos-2 cells; however, the exact relationship between L/B/K ALP or TNSALP and DATS should be clearly described.

In summary, the results of this study indicate that DATS has the ability to suppress cell proliferation of Saos-2 cells by blocking cell cycle progression and inducing apoptosis in a dose-dependent and time-dependent manner. Furthermore, the proteomic data provide novel insight into a massive response of protein expression in Saos-2 cells induced by DATS, and show that some of DATS-sensitive proteins are related to cell cycle or apoptosis. Therefore, it seems reasonable to conclude that DATS exert multiple stimuli to several biological pathways, which could elucidate the anticarcinogenic effects of DATS. Moreover, the DATS-sensitive proteins in our study might be applied as therapeutic targets for gene therapy of osteosarcoma. The proteomic study on Saos-2 cells treated with DATS confirmed that DATS could exert its anticarcinogenic effects on human osteosarcoma cell line that is not from glandular organ or epithelial tissue. However, the DATS-sensitive proteins in Saos-2 cells and its molecular mechanisms should be accurately studied using other experimental methods.

References

1 Rivlin RS. Historical perspective on the use of garlic. *J Nutr* 2001; **131**:951s–954s.
2 Manson MM. Cancer prevention–the potential for diet to modulate molecular signaling. *Trends Mol Med* 2003; **9**:11–18.
3 Yu FL, Bender W, Fang Q, Ludeke A, Welch B. Prevention of chemical carcinogen DNA binding and inhibition of nuclear RNA polymerase activity by organosulfur compounds as the possible mechanisms for their anticancer initiation and proliferation effects. *Cancer Detect Prev* 2003; **27**:370–379.
4 Guyonnet D, Belloir C, Suschetet M, Siess MH, Le Bon AM. Mechanisms of protection against aflatoxin B (1) genotoxicity in rats treated by organosulfur compounds from garlic. *Carcinogenesis* 2002; **23**:1335–1341.
5 Hu X, Benson PJ, Srivastava SK, Mack LM, Xia H, Gupta V, *et al.* Glutathione S-transferases of female A/J mouse liver and forestomach and their differential induction by anticarcinogenic organosulfides from garlic. *Arch Biochem Biophys* 1996; **336**:199–214.
6 Andorfer JH, Tchaikovskaya T, Listowsky I. Selective expression of glutathione S-transferase genes in the murine gastrointestinal tract in response to dietary organosulfur compounds. *Carcinogenesis* 2004; **25**:359–367.
7 Tsai CW, Chen HW, Yang JJ, Sheen LY, Lii CK. Diallyl disulfide and diallyl trisulfide up-regulate the expression of the π class of glutathione S-transferase via an AP-1-dependent pathway. *J Agric Food Chem* 2007; **55**:1019–1026.
8 Xiao D, Herman-Antosiewicz A, Antosiewicz A, Xiao H, Brisson M, Laz JS, *et al.* DATS-induced cell cycle arrest in human prostate cancer cells is caused by reactive oxygen species dependent destruction and hyperphosphorylation of Cdc25C. *Oncogene* 2005; **24**:6256–6268.
9 Herman-Antosiewicz A, Singh SV. Checkpoint kinase 1 regulates diallyl trisulfide-induced mitotic arrest in human prostate cancer cells. *J Biol Chem* 2005; **280**:28519–28528.
10 Xiao D, Choi S, Johnson DE, Vogel VG, Johnson CS, Trump DL, *et al.* DATS-induced apoptosis in human prostate cancer cells involves c-Jun N-terminal kinase and extracellular signal regulated kinase-mediated phosphorylation of Bcl-2. *Oncogene* 2004; **23**:5594–5606.
11 Xiao D, Singh SV. Diallyl trisulfide, a constituent of processed garlic, inactivates Akt to trigger mitochondrial translocation of BAD and caspase-mediated apoptosis in human prostate cancer cells. *Carcinogenesis* 2006; **27**:533–540.
12 Herman-Antosiewicz A, Singh SV. Signal transduction pathways leading to cell cycle arrest and apoptosis induction in cancer cells by *Allium* vegetable-derived organosulfur compounds: a review. *Mutat Res* 2004; **555**:121–131.
13 Takashi H, Tomomi F, Jun O, Yoshimasa I, Hajime S, Taiichiro S, *et al.* Diallyl trisulfide suppresses the proliferation and induces apoptosis of human colon cancer cells through oxidative modification of β–tubulin. *J Biol Chem* 2005; **280**:41487–41493.
14 Li N, Guo R, Li W, Shao J, Li S, Zhao K, *et al.* A proteomic investigation into a human gastric cancer cell line BGC823 treated with diallyl trisulfide. *Carcinogenesis* 2006; **27**:1222–1231.
15 Kang JH, Park KK, Lee IS, Magae JJ, Ando Kim CH, Chang YC. Proteome analysis of responses to ascochlorin in a human osteosarcoma cell line by 2-D gel electrophoresis and MALDI-TOF MS. *J Proteome Res* 2006; **5**:2620–2631.

16 Posadas EM, Simpkins F, Liotta LA, MacDonald C, Kohn EC. Proteomic analysis for the early detection and rational treatment of cancer–realistic hope? *Ann Oncol* 2005; **16**:16–22.
17 Li ZP, Michael K, Stefan M, Nikica M, Michael OG, Brigitte MP. Proteomic analysis of the E2F1 response in p53-negative cancer cells: new aspects in the regulation of cell survival and death. *Proteomics* 2006; **6**:5735–5745.
18 Spreafico A, Frediani B, Capperucci C, Chellini F, Paffetti A, Ambrosio G, *et al*. A proteomic study on human osteoblastic cells proliferation and differentiation. *Proteomics* 2006; **6**:3520–3532.
19 Jakubikova J, Sedlak J. Garlic-derived organosulfides induce cytotoxicity, apoptosis, cell cycle arrest and oxidative stress in human colon carcinoma cell lines. *Neoplasma* 2006; **53**:191–199.
20 Wu CC, Chung JG, Tsai SJ, Yang JH, Sheen LY. Differential effects of allyl sulfides from garlic essential oil on cell cycle regulation in human liver tumor cells. *Food Chem Toxicol* 2004; **42**:1937–1947.
21 Zwickl P, Voges D, Baumeister W. The proteasome: a macromolecular assembly designed for controlled proteolysis. *Phil Trans R Soc Lond B Biol Sci* 1999; **354**:1501–1511.
22 Rajkumar SV, Richardson PG, Hideshima T, Anderson KC. Proteasome inhibition as a novel therapeutic target in human cancer. *J Clin Oncol* 2005; **23**:630–639.
23 Codony-Servat J, Tapia MA, Bosch M, Oliva C, Domingo-Domenech J, Mellado B, *et al*. Differential cellular and molecular effects of bortezomib, a proteasome inhibitor, in human breast cancer cells. *Mol Cancer Ther* 2006; **5**:665–675.
24 Laurent N, Bouard S, Guillamo JS, Christov C, Zini R, Jouault H, *et al*. Effects of the proteasome inhibitor ritonavir on glioma growth in vitro and in vivo. *Mol Cancer Ther* 2004; **3**:129–136.
25 Bazzaro M, Lee MK, Zoso A, Wanda HS, Santillan A, Shih IM, *et al*. Ubiquitin–proteasome system stress sensitizes ovarian cancer to proteasome inhibitor-induced apoptosis. *Cancer Res* 2006; **66**:3754–3763.
26 Paramio JM, Casanova ML, Segrelles C, Mittnacht S, Lane EB, Jorcano JL. Modulation of cell proliferation by cytokeratins k10 and k16. *Mol Cell Biol* 1999; **19**:3086–3094.
27 Paramio JM, Segrelles C, Ruiz S, Jorcano JL. Inhibition of protein Kinase B (PKB) and PKCζ mediates keratin K10-induced cell cycle arrest. *Mol Cell Biol* 2001; **21**:7449–7459.
28 Paramio JM, Jorcano JL. Role of protein kinases in the in vitro differentiation of human epidermal HaCaT cells. *Br J Dermatol* 1997; **137**:44–50.
29 Xiao D, Lew KL, Kim YA, Zeng Y, Hahm ER, Dhir R, *et al*. Diallyl trisulfide suppresses growth of PC-3 human prostate cancer xenograft in vivo in association with Bax and Bak induction. *Clin Cancer Res* 2006; **12**:6836–6843.
30 Lee AS. GRP78 induction in cancer: therapeutic and prognostic implications. *Cancer Res* 2007; **67**:3496–3499.
31 Song MS, Park YK, Lee JH, Park K. Induction of glucose-regulated protein 78 by chronic hypoxia in human gastric tumor cells through a protein kinase C-ε/ERK/AP-1 signaling cascade. *Cancer Res* 2001; **61**:8322–8330.
32 Ermakova SP, Kang BS, Choi BY, Choi HS, Schuster TF, Ma WY, *et al*. (–)–Epigallocatechin gallate overcomes resistance to etoposide-induced cell death by targeting the molecular chaperone glucose-regulated protein 78. *Cancer Res* 2006; **66**:9260–9269.
33 Davidson DJ, Haskell C, Majest S, Kherzai A, Egan DA, Walter KA, *et al*. Kringle 5 of human plasminogen induces apoptosis of endothelial and tumor cells through surface-expressed glucose-regulated protein 78. *Cancer Res* 2005; **65**:4663–4672.
34 Ranganathan AC, Zhang L, Adam AP, Aguirre-Ghiso JA. Functional coupling of p38-induced up-regulation of BiP and activation of RNA-dependent protein kinase-like endoplasmic reticulum kinase to drug resistance of dormant carcinoma cells. *Cancer Res* 2006; **66**:1702–1711.
35 Gonzalez-Gronow M, Cuchacovich M, Llanos C, Urzua C, Gawdi G, Pizzo SV. Prostate cancer cell proliferation in vitro is modulated by antibodies against glucose-regulated protein 78 isolated from patient serum. *Cancer Res* 2006; **66**:11424–11431.
36 Gupta P, Walter MR, Su ZZ, Lebedeva IV, Emdad L, Randolph A, *et al*. BiP/GRP78 is an intracellular target for MDA-7/IL-24 induction of cancer-specific apoptosis. *Cancer Res* 2006; **66**:8182–8191.
37 Bagatell R, Whitesell L. Altered Hsp90 function in cancer: A unique therapeutic opportunity. *Mol Cancer* 2004; **3**:1021–1030.
38 Beere HM, Wolf BB, Cain K. Heat-shock protein 70 inhibits apoptosis by preventing recruitment of procaspase-9 to the Apaf-1 apoptosome. *Nat Cell Biol* 2000; **2**:469–475.
39 Saleh A, Srinivasula SM, Balkir L, Robbins PD, Alnemri ES. Negative regulation of the Apaf-1 apoptosome by Hsp70. *Nat Cell Biol* 2000; **2**:476–483.
40 Rao JY, Li N. Microfilament actin remodeling as potential target for cancer drug development. *Curr Cancer Drug Targets* 2004; **4**:345–354.
41 Verrills NM, Pouha ST, Liu ML, Liaw TY, Larsen MR, Ivery MT, *et al*. Alterations in γ-actin and tubulin-targeted drug resistance in childhood leukemia. *J Natl Cancer Inst* 2006; **98**:1363–1374.
42 Hattori M, Minato N. Rap1 GTPase: functions, regulation, and malignancy. *J Biochem* 2003; **134**:479–484.
43 Gao L, Feng Y, Bowers R, Becker-Hapak M, Gardner J, Council L, *et al*. Ras-associated protein-1 regulates extracellular signal-regulated kinase activation and migration in melanoma cells: two processes important to melanoma tumorigenesis and metastasis. *Cancer Res* 2006; **66**:7880–7888.
44 Itoh M, Nelson CM, Myers CA, Bissell MJ. Rap1 integrates tissue polarity, lumen formation, and tumorigenic potential in human breast epithelial cells. *Cancer Res* 2007; **7**:4759–4766.
45 De Falco V, Castellone MD, De Vita G, Cirafici AM, Hershman JM, Guerrero C, *et al*. RET/papillary thyroid carcinoma oncogenic signaling through the Rap1 small GTPase. *Cancer Res* 2007; **67**:381–390.
46 Park EK, Kwon KB, Park KI, Park BH, Jhee EC. Role of Ca(2+) in diallyl disulfide-induced apoptosis cell death of HCT-15 cells. *Exp Mol Med* 2002; **34**:250–257.
47 Sakamoto K, Lawson LD, Milner JA. Allyl sulfides from garlic suppress the in vitro proliferation of human A549 lung tumor cells. *Nutr Cancer* 1997; **29**:152–156.
48 Lee AS. Mammalian stress response: induction of the glucose-regulated protein family. *Curr Opin Cell Biol* 1992; **4**:267–273.
49 Michalak M, Corbett EF, Mesaeli N, Nakamura K, Opas M. Calreticulin: one protein, one gene, many functions. *J Biochem* 1999; **344**:281–292.
50 Arnaudeau S, Frieden M, Nakamura K, Castelbou C, Michalak M, Demaurex N. Calreticulin differentially modulates calcium uptake and release in the endoplasmic reticulum and mitochondria. *J Biol Chem* 2002; **277**:46696–46705.
51 Kageyama K, Ihara Y, Goto S, Urata Y, Toda G, Yano K, *et al*. Overexpression of calreticulin modulates protein kinase B/Akt signaling to promote apoptosis during cardiac differentiation of cardiomyoblast H9c2 cells. *J Biol Chem* 2002; **277**:19255–19264.
52 Okunaga T, Urata Y, Goto S, Matsuo T, Mizota S, Tsutsumi K, *et al*. Calreticulin, a molecular chaperone in the endoplasmic reticulum, modulates radiosensitivity of human glioblastoma U251MG cells. *Cancer Res* 2006; **66**:8662–8671.
53 Mesaeli N, Phillipson C. Impaired p53 expression, function, and nuclear localization in calreticulin-deficient cells. *Mol Biol Cell* 2004; **15**:1862–1870.
54 Yoon WH, Song IS, Lee BH, Jung YJ, Kim TD, Li G, *et al*. Differential regulation of vimentin mRNA by 12-O-tetradecanoylphorbol 13-acetate and all-trans-retinoic acid correlates with motility of Hep 3B human hepatocellular carcinoma cells. *Cancer Lett* 2004; **203**:99–105.
55 Wu M, Bai X, Xu G, Wei J, Zhu T, Zhang Y, *et al*. Proteome analysis of human androgen-independent prostate cancer cell lines: variable metastatic potentials correlated with vimentin expression. *Proteomics* 2007; **7**:1973–1983.
56 Byun Y, Chen F, Chang R, Trivedi M, Green KJ, Cryns VL. Caspase cleavage of vimentin disrupts intermediate filaments and promotes apoptosis. *Cell Death Differ* 2001; **8**:443–450.
57 Singh S, Sadacharan S, Su S, Belldegrun A, Persad S, Singh G. Overexpression of vimentin: role in the invasive phenotype in an androgen independent model of prostate cancer. *Cancer Res* 2003; **63**:2306–2311.
58 Kaya B, Mena H, Miettinen M, Rushing EJ. Alpha-internexin expression in medulloblastomas and atypical teratoid–rhabdoid tumors. *Clin Neuropathol* 2003; **22**:215–221.
59 Chien CL, Liu TC, Ho CL, Lu KS. Overexpression of neuronal intermediate filament protein α-internexin in PC12 cells. *J Neurosci Res* 2005; **80**:693–706.
60 Manara MC, Baldini N, Serra M, Lollini PL, De Giovanni C, Vaccari M, *et al*. Reversal of malignant phenotype in human osteosarcoma cells transduced with the alkaline phosphatase gene. *Bone* 2000; **26**:215–220.
61 Orimot H, Shimada T. Regulation of the human tissue-nonspecific alkaline phosphatase gene expression by all-trans-retinoic acid in SaOS-2 osteosarcoma cell line. *Bone* 2005; **36**:866–876.
62 Tsai LC, Hung MW, Chen YH, Su WC, Chang GG, Chang TC. Expression and regulation of alkaline phosphatases in human breast cancer MCF-7 cells. *Eur J Biochem* 2000; **267**:1330–1333.
63 Namba T, Hoshino T, Tanaka K, Tsutsumi S, Ishihara T, Mima S, *et al*. Up-regulation of 150-kDa oxygen-regulated protein by celecoxib in human gastric carcinoma cells. *Mol Pharmacol* 2007; **71**:860–870.
64 Harada T, Harada C, Wang YL, Osaka H, Amanai K, Tanaka K, *et al*. Role of ubiquitin carboxy terminal hydrolase-l1 in neural cell apoptosis induced by ischemic retinal injury in vivo. *Am J Pathol* 2004; **164**:59–64.